processes

MDPI

Article

Aristolochic Acid I Adsorption onto Activated Carbon: Kinetics, Equilibrium, and Thermodynamic Studies

Maria-Alexandra Pricop [1,2], Adina Negrea [1], Mihaela Ciopec [1], Ioan Bogdan Pascu [3,*], Camelia Oprean [2,4,5], Alexandra Teodora Lukinich-Gruia [2,*], Iustina-Mirabela Cristea [2], Alexandra Ivan [2,6], Virgil Păunescu [2,6] and Călin Adrian Tatu [2,6]

1 Faculty of Chemical Engineering, Biotechnologies and Environmental Protection, Politehnica University Timisoara, Victoriei Square, No. 2, 300006 Timișoara, Romania; maria.pricop@student.upt.ro (M.-A.P.); adina.negrea@upt.ro (A.N.); mihaela.ciopec@upt.ro (M.C.)
2 OncoGen Centre, Clinical County Hospital "Pius Branzeu", Blvd. Liviu Rebreanu 156, 300723 Timisoara, Romania; camelia.oprean@umft.ro (C.O.); miracristea82@gmail.com (I.-M.C.); ivan.alexandra@umft.ro (A.I.); vpaunescu@umft.ro (V.P.); tatu.calin@umft.ro (C.A.T.)
3 Renewable Energy Research Institute—ICER, Politehnica University of Timisoara, 138 Gavril Musicescu Street, 300501 Timisoara, Romania
4 Faculty of Pharmacy, "Victor Babeș" University of Medicine and Pharmacy of Timișoara, E. Murgu Sq., No. 2, 300041 Timișoara, Romania
5 Center for Drug Data Analysis, Cheminformatics and the Internet of Medical Things, "Victor Babeș" University of Medicine and Pharmacy, Timișoara, E. Murgu Sq., No. 2, 300041 Timisoara, Romania
6 Department of Functional Sciences, Center of Immuno-Physiology (CIFBIOTEH), University of Medicine and Pharmacy "Victor Babes", Eftimie Murgu Sq. 2, 300041 Timisoara, Romania
* Correspondence: ioan.pascup@upt.ro (I.B.P.); alexandra.gruia@hosptm.ro (A.T.L.-G.)

Abstract

The removal of phytotoxins from herbal preparations is important due to evidence linking exposure to aristolochic acid I (AAI), a toxin found in *Aristolochiaceae* species, with certain kidney diseases. This study evaluates the effectiveness of activated carbon (AC) in removing AAI from aqueous solutions and determines the optimal conditions for the process, which are necessary for accurate kinetic, thermodynamic, and equilibrium analyses. After establishing the best conditions for the adsorption reaction (pH > 6; solid/liquid ratio (S:L) = 0.1 g adsorbent: 25 mL AAI solution; contact time 120 min; temperature = 298 K, AAI initial concentration (Ci) = 150 mg/L), a maximum adsorption capacity of 10.67 mg/g was obtained. Quantitative analysis of AAI was performed using UV-VIS spectrophotometry. Experiments on kinetics, thermodynamics, and adsorption isotherms were carried out. The findings showed that the process adheres to pseudo-second-order kinetics and is spontaneous and endothermic and takes place at the interface between the adsorbent and adsorbate. The equilibrium data fits the Sips isotherm model with a regression coefficient close to 1. The findings indicate that AC is an effective material for the removal of AAI by adsorption from an aqueous solution.

Keywords: aristolochic acid I; phytotoxin; activated charcoal removal; kinetic studies; thermodynamic; equilibrium studies

check for updates

Academic Editors: Alejandro Regalado-Méndez, Reyna Natividad and Rubi Romero

Received: 15 September 2025
Revised: 19 October 2025
Accepted: 20 October 2025
Published: 23 October 2025

Citation: Pricop, M.-A.; Negrea, A.; Ciopec, M.; Pascu, I.B.; Oprean, C.; Lukinich-Gruia, A.T.; Cristea, I.-M.; Ivan, A.; Păunescu, V.; Tatu, C.A. Aristolochic Acid I Adsorption onto Activated Carbon: Kinetics, Equilibrium, and Thermodynamic Studies. *Processes* **2025**, *13*, 3397. https://doi.org/10.3390/pr13113397

Copyright: © 2025 by the authors. Licensee MDPI, Basel, Switzerland. This article is an open access article distributed under the terms and conditions of the Creative Commons Attribution (CC BY) license (https://creativecommons.org/licenses/by/4.0/).

1. Introduction

The scientific community's attention to the link between aristolochic acids (AAs), the main toxic compounds in the *Aristolochiaceae* family, and chronic kidney disease (CKD) began in 1992, following an unfortunate medical event in Belgium. At that time, an association was observed between the use of Chinese herbal weight loss treatments and a

peculiar form of renal failure and urothelial cancer, later called Chinese Herbs Nephropathy (CHN) [1]. The weight loss pills accidentally contained *Aristolochia fangchi* plant parts, rich in AAs [2].

Subsequently, studies have indicated the consumption of various forms of plants from the *Aristolochiaceae* family by patients with renal failure in different regions of the world, thus reclassifying CHN as Aristolochic Acid Nephropathy (AAN). At the same time, in the Balkan region of Europe, the hypothesis of AA involvement as a causing factor of Balkan endemic nephropathy (BEN) was formulated and subsequently consolidated, following the accumulation of AA in natural sources (soil, water, air) [3].

Today, the well-established carcinogenic, mutagenic, and nephrotoxic nature of AAs is well documented [4], which limits the clinical applications of herbal treatments containing these compounds. Also, environmental contamination with this nephrotoxins is a current problem [3]. To lower the number of AAN and BEN cases, it is important to reduce exposure to this toxin. Developing ways to remove AAs from contaminated herbal remedies and limiting exposure through the food chain are key steps [1,2].

In recent years, researchers have focused on identifying selective and sensitive methods for the analysis of AAs, applied to natural plants, drugs, and environmental and biological samples, as well as their removal from herbal medicines and the environment, by identifying efficient removal methods or synthesizing new materials with AA removal/isolation properties [5,6].

The current methods proposed by researchers for the removal of AAs are microbiological methods, physical adsorption separation methods and chemical methods [3]. Regarding the detoxification of materials containing aristolochic acid I (AAI), microbial degradation [4] offers a low-cost and environmentally friendly alternative to conventional extraction methods such as solid phase extraction [5–9], electromembrane extraction [10], QuEChERS [11,12], and supercritical fluid extraction [13]—although it requires a longer processing time—while advanced oxidation technologies have also been explored for environmental AAI degradation [14]. Having remarkable adsorption properties, activated carbon (AC) is an essential material, with various applications in environmental protection, air and water purification, and healthcare. Due to its effectiveness and versatility in capturing and removing a wide range of contaminants, AC is widely used today in various industries [15].

This study proposes analyzing the efficiency of a simple and accessible method to remove aristolochic acid I (AAI), a predominant compound among aristolochic acids (AAs). The novelty consists in the use of activated carbon (AC) for the potential removal of AAI from aqueous solutions by adsorption on a cheap, common and environmentally friendly material, whose advantageous features are the large contact surface and high porosity. In addition, this study provides a clear elucidation of the adsorption mechanism of AAI onto AC, which stands out as a novel contribution within the context of removing AAI. For environmental decontamination and remediation, it is essential to understand the AAI adsorption mechanism. For quantitative determination of AAI in the samples, UV-VIS spectroscopy was used, while the adsorption mechanism of AAI by AC was elucidated through complete kinetic, thermodynamic and equilibrium evaluations. Taken together, the data confirms that AC is an efficient and promising material for capturing and removing AAI from various samples for the purpose of detoxification and environmental remediation.

2. Materials and Methods

2.1. Study Design

This study investigates the adsorption of aristolochic acid I (AAI) onto activated carbon (AC). Key parameters including pH, contact time, adsorbent dose, and temperature were optimized using systematic kinetic, thermodynamic, and equilibrium analyses. The

aim is to establish an efficient method for removing this toxic compound from aqueous solutions. The reaction mechanism was also determined [16,17].

2.2. Reagents and Chemicals

Aristolochic acid I powder used as the adsorbate was purchased from Sigma-Aldrich (Merck Group, Darmstadt, Germany) with a purity of ≥97%, while the adsorbent material, powdered activated carbon (mesh size 100), was obtained from ROTH (Carl Roth GmbH + Co. KG, Karlsruhe, Germany); all other chemicals used, including solvents and reagents, were of analytical grade and procured from reliable commercial suppliers.

2.3. AAI Detection

The AAI was analyzed using ultraviolet–visible spectrometry (UV-VIS). AAI absorption spectra were recorded in a 10 mm quartz cell (Hellma Analytics, Müllheim, Germany), from 200 to 600 nm, with a Varian Cary 50 UV–VIS spectrophotometer (Varian Inc., Palo Alto, CA, USA). To determine the wavelength at which AAI absorbs, the UV-VIS spectrum was recorded with Cary winUV software (Varian Inc., Palo Alto, CA, USA) for a 10 mg/L solution, dissolved in ethanol (ChimReactiv SRL, București, Romania) at 20 °C.

2.4. Adsorption Studies

Kinetic, thermodynamic, and equilibrium adsorption studies were conducted on activated charcoal to evaluate its removal efficiency of aristolochic acid, elucidate the adsorption mechanism, determine the maximum adsorption capacity, and identify the optimal conditions for effective toxin removal after an adapted method [16]. The pH, solid-to-liquid (S:L) ratio, temperature, and contact time are essential variables, and they order the adsorption speed and the total adsorption capacity. By varying these parameters the adsorption mechanism can be understood, boosting the detoxification efficiency. Also, the adsorption kinetics and equilibrium are dictated by these parameters. To deliver insights into the adsorption rate, kinetic analysis was further provided using a pseudo-second-order model. Optimizing these variables is essential to accurately model the kinetics and isotherms, thereby gaining a clear understanding of the adsorption mechanism and enhancing detoxification efficiency under controlled conditions. These parameters significantly impact adsorption kinetics and equilibrium. Kinetic analysis was further refined using pseudo-second-order modeling, delivering insights into the adsorption rate and characteristics. Thermodynamic evaluation indicated that the adsorption of AAI on AC is spontaneous and endothermic, reflecting favorable conditions for efficient removal. Equilibrium aspects were explored through the application of the Sips isotherm model, enabling precise quantification of adsorption capacity across different conditions.

2.4.1. Influence of pH

A study was conducted to investigate the influence of the pH of the AAI solution on the adsorption process of coal powdered activated carbon. The pH of the samples was modified using solutions of 0.05–2 N NaOH and 0.05–2 N HNO_3. The pH range was set between 1 and 12. A 10 mg/L AAI solution was prepared by diluting the stock solution with distilled water. A quantity of 0.2 g AC was accurately weighed for each sample, over which 25 mL of the desired pH AAI solution was added. The samples were then stirred for 60 min in a water bath with a thermostat. After filtration, the residual concentration of AAI in the filtrate was determined by UV-VIS spectrometry at 320 nm with a Varian Carry 50 UV-VIS spectrophotometer.

2.4.2. Influence of Solid/Liquid Ratio

Another parameter that was investigated to ascertain the efficacy of the AC adsorption process was the solid/liquid ratio (S:L). For this purpose, different amounts of solid material (0.05; 0.1; 0.15; 0.2; 0.3; 0.4; 0.5 g) were weighed and placed in contact with a 25-milliliter solution of AAI at a concentration of 10 mg/L and a pH of 6. Samples were kept in contact for 120 min (adsorption equilibrium time) in a thermostated and stirred water bath at 298 K, with a rotation speed (shaking rate) of 200 rpm. Subsequently, the samples were filtered, and the AAI residual concentration was analyzed by UV-VIS spectrophotometry.

2.4.3. Influence of Temperature and Contact Time

The AC adsorption capacity was investigated through contact time and temperature. Therefore, 0.2 g of the material was accurately weighed, and 25 mL of 10 mg/L AAI solution was added. The AC was maintained in contact with the AAI solution for varying periods of time (30, 45, 60, 90, 120, and 180 min) and at different temperatures (298 K, 308 K, 318 K, and 328 K) in a thermostated and stirred water bath at 200 rpm rotational speed. Subsequently, the samples were filtered to analyze the AAI residual concentration with UV-VIS spectrophotometry.

2.4.4. Influence of the Initial Concentration

The influence of the AAI initial concentration (Ci AAI) on the equilibrium concentration, Ci AAI varied in the range of 5 to 160 mg/L AAI, starting with a stock solution of 1 g/L. The solutions were prepared using distilled water. Adsorption studies were conducted in accordance with the previously established conditions, namely static, using a thermostated bath at 200 rpm, pH > 6, time 120 min, temperature 298 K, ratio S:L = 0.2 g:25 mL, sample volume 25 mL. The filtrate was analyzed for AAI residual concentration (Cf AAI) using UV-VIS spectrophotometry.

The material adsorption capacity, q_e (mg/g), was determined using equation [18]:

$$q_e = \frac{(C_0 - C_f)V}{m} \quad (1)$$

where C_0 is the original concentration of AAI in the solution, (mg/L); C_f is the residual concentration of AAI in solution, (mg/L); V is the volume of solution, (L); and m is the mass of adsorbent material, (g).

2.5. Kinetic Studies

Kinetic investigation was completed using two models: the pseudo-first-order model introduced by Lagergren [19] and the pseudo-second-order model developed by Ho and McKay [20].

The experimental data were constructed using the pseudo-first-order model, following the next mathematical expression [19]:

$$\ln(q_e - q_t) = \ln q_e - k_1 t \quad (2)$$

where q_e represents the amount of AAI adsorbed per unit mass of AC at equilibrium, while q_t denotes the amount adsorbed at a specific time (t). The parameter k_1 is the rate constant associated with the pseudo-first-order adsorption process.

An equation that describes the pseudo-second-order kinetic has been used [20]:

$$\frac{t}{q_t} = \frac{1}{k_2 q_e^2} + \frac{t}{q_e} \quad (3)$$

To analyze the experimental data, the linear forms of both kinetic models were used. The pseudo-second-order kinetic linear model is obtained after the t/q_t (time dependent) was plotted against the three working temperatures.

2.6. Thermodynamic Studies

The effect of temperature and thermodynamic parameters were observed for the adsorption process of AAI on AC, namely Gibbs free energy, ΔG_0 [21], enthalpy, ΔH_0 [22], entropy, ΔS_0 and the activation energy, E_a [21].

The Gibbs free energy was estimated by applying the equations below [21]:

$$\Delta G^0 = -RT\ln K_d \quad (4)$$

where

$$K_d = \frac{C_{A_e}}{C_e} \quad (5)$$

where C_{A_e} is the AAI equilibrium concentration on adsorbent (mg/g); C_e is the AAI equilibrium concentration in the solution (mg/g).

$$\text{So,} \qquad \ln K_d = \frac{\Delta S^0}{R} - \frac{\Delta H^0}{RT} \quad (6)$$

where K_d is the equilibrium constant; ΔS^0 is the entropy standard variation (J mol^{-1} k^{-1}); ΔH^0 is the enthalpy standard variation (kJ mol^{-1}); R is the ideal gas constant (8.314 J mol^{-1} K^{-1}); and T is the absolute temperature (K).

According to the Arrhenius equation, the activation energy, E_a, can be calculated as a result of the following expression [23]:

$$\ln k_2 = \ln A - \frac{E_a}{RT} \quad (7)$$

where k_2 is the speed constant (g/min·mg); A is the Arrhenius constant (g·min/mg); E_a is the Activation energy (kJ/mol); T is the absolute temperature (K); and R is the ideal gas constant (8.314 J/mol·K).

2.7. Equilibrium Studies

The experimental results were explored by fitting them to the Langmuir [22], Freundlich [24], and Sips [25] isotherms. The nonlinear form of Langmuir isotherm is used to describe adsorption on uniform surfaces, and the specific calculation formula is represented [26]:

$$q_e = \frac{q_{max} K_L C_f}{1 + K_L C_f} \quad (8)$$

where q_e is the maximum absorption capacity (mg/g); C_f is the equilibrium concentration or final concentration of AAI in solution (mg/L); q_{max} is the Langmuir maximum adsorption capacity (mg/g); and K_L is the Langmuir constant.

The Freundlich isotherm describes a heterogeneous adsorption surface [24]. The nonlinear form of the Freundlich isotherm equation [24] is as follows:

$$q_e = K_F C_f^{1/n_f} \quad (9)$$

where q_e is the maximum absorption capacity (mg/g); C_f is the equilibrium concentration or final concentration of AAI in solution (mg/g); and K_F and n_F are the isotherm constants associated with the adsorbent's relative capacity and the intensity of the adsorption.

These two models, Langmuir and Freundlich, give a third nonlinear Sips model [25,27]:

$$q_e = \frac{q_s K_s C_e^{1/n_s}}{1 + K_s C_e^{1/n_s}} \quad (10)$$

where q_s is the maximum absorption capacity (mg/g); K_s is the adsorption capacity coefficient; and n_s is the heterogeneity factor.

3. Results

3.1. Detection of AAI

After scanning a standard solution of AAI, in the wavelength range 200–600 nm, the absorption spectrum of AAI was obtained. From Figure 1, three absorption peaks can be observed at 250 nm, 320 nm, and 392 nm, respectively, specific for AAI, and comparable to those in the literature [28,29]. Because the most intense and stable peak was obtained at 320 nm, when compared with the absorption peaks observed at 250 and 392 nm, the analysis was performed at this wavelength, supporting a fine signal-to-noise ratio.

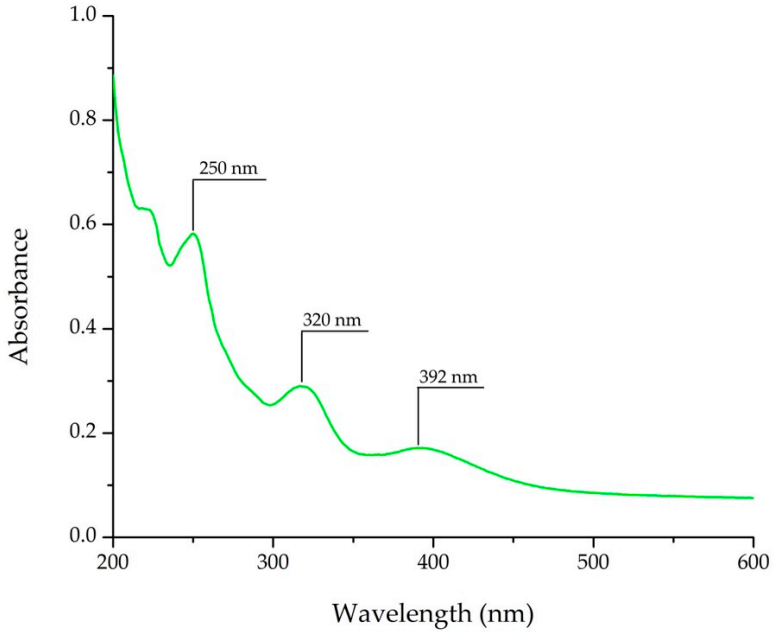


Figure 1. The ultraviolet spectrum for AAI.

3.2. Adsorption Studies and Kinetic, Thermodynamic, and Equilibrium Studies

The following sections present comprehensive results that shed light on the adsorption mechanism, capacity, and efficiency under the influence of pH, solid-to-liquid ratio, temperature, and contact time.

3.2.1. pH Influence on the Adsorption Process

It is well established that pH is a key factor influencing the adsorption process. The pH changes in the aqueous AAI solution influence the adsorption performance of AC (Figure 2).

After the variation in the pH, it was established that the solution's pH should remain at 6. The adsorption capacity of AC increases as pH rises from 1 to 6 but stabilizes and remains approximately constant (~0.7 mg/g) for pH values above 6 (Figure 3).

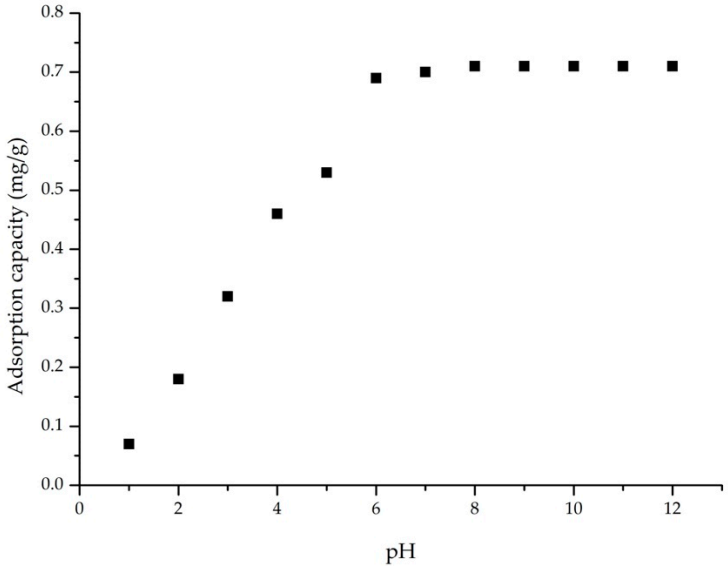


Figure 2. pH influence on the adsorption process (condition: contact time, 60 min; 298 K; V = 25 mL; Ci = 10 mg/L AAI; ratio S:L = 0.2 g:25 mL).

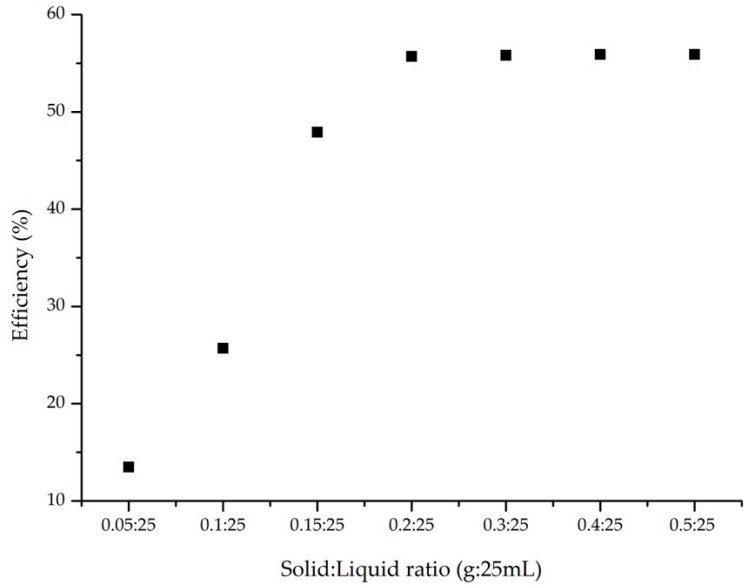


Figure 3. Influence of S:L ratio (condition: contact time, 60 min; 298 K; V = 25 mL; Ci = 10 mg/L AAI; pH = 6).

3.2.2. Influence of Solid/Liquid Ratio

The solid/liquid (S:L) ratio is another crucial parameter for optimizing adsorption conditions. In this study, Figure 3 illustrates the effect of the S:L ratio on the adsorption efficiency.

From the experimental data obtained, it was found that with an increasing S:L ratio, the efficiency of the adsorption process increases, reaching a maximum efficiency of approximately 55% at an S:L ratio of 0.2 g to 25 mL.

3.2.3. Influence of Contact Time and Temperature

To track how contact time and temperature affect the capacity of the sorbent, a plot was generated (Figure 4). When the interaction between AC and AAI increases, the adsorption capacity rises from 0.77 to 0.9 mg/g, with variations depending on the temperature range studied (298 K to 328 K).

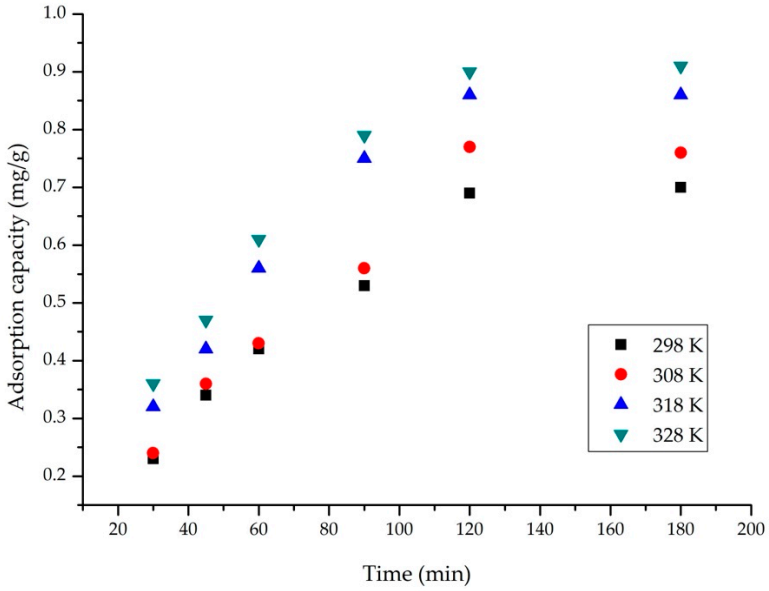
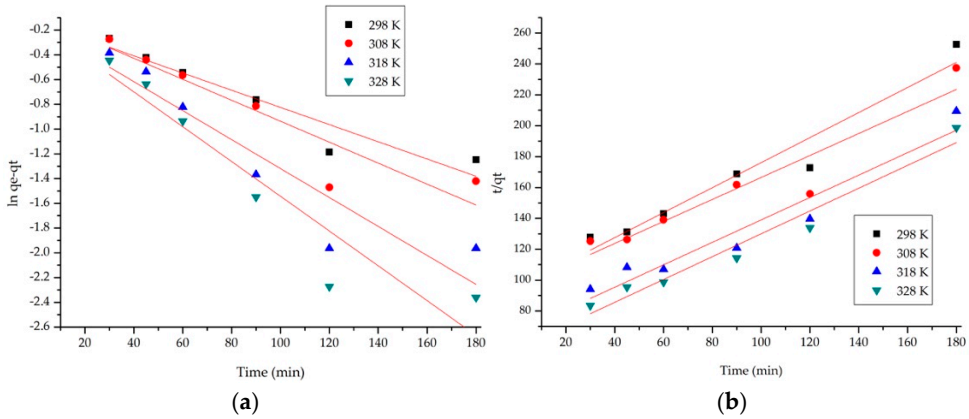


Figure 4. Influence of the contact time and temperature (condition: contact time, 30–180 min; pH = 6; V = 25 mL; Ci = 10 mg/L AAI; ratio S:L = 0.2 g:25 mL).

As temperature has a minimal effect on the adsorption process, operation at high temperatures is therefore not required, so the experiments were carried out at 298 K for 120 min.

3.2.4. Kinetic Studies

Kinetic analyses were performed to demonstrate the adsorption process mechanism. The rate constant for the pseudo-first-order kinetic model was determined from the linear plot of ln ($q_e - q_t$) versus time (Figure 5a), while the rate constant for the pseudo-second-order kinetic model was obtained from the linear plot of t/q_t versus time (Figure 5b). The red lines are used to evaluate how well the experimental data fit the theoretical model (Figure 5a,b). By examining the rate constants and the corresponding regression coefficients (R^2) (Table 1), the most suitable kinetic model describing the adsorption process can be determined.



(**a**) (**b**)

Figure 5. Kinetic models: (**a**) pseudo− first− order model; (**b**) pseudo− second− order model. The red lines are used to evaluate how well the experimental data fit the theoretical model.

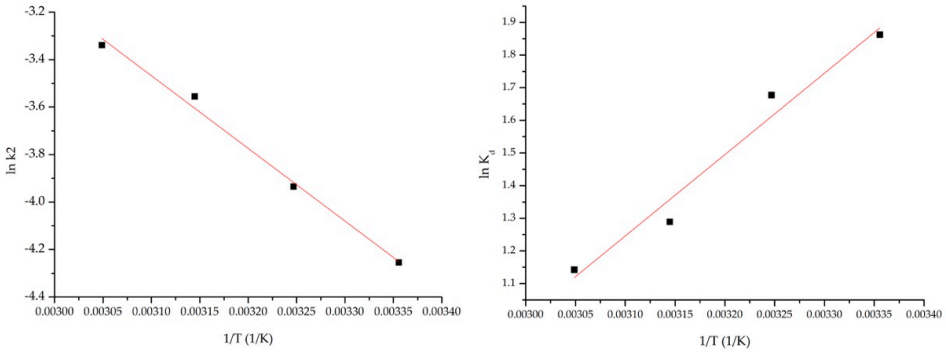
Table 1. Kinetic parameters for the adsorption of AAI onto AC.

Pseudo-First-Order Model (Lagergren Model)				
Temperature (K)	$q_{e,\,exp}$ (mg·g^{-1})	k_1 (min^{-1})	$q_{e,\,calc}$ (mg·g^{-1})	R^2
298	0.69	0.0069	1.14	0.9109
308	0.77	0.0081	1.10	0.8618
318	0.86	0.0117	1.16	0.8710
328	0.89	0.0141	1.15	0.9750
Pseudo-Second-Order Model (Ho and McKay Model)				
Temperature (K)	$q_{e,\,exp}$ (mg·g^{-1})	k_2 (min^{-1})	$q_{e,\,calc}$ (mg·g^{-1})	R^2
298	0.69	0.0142	1.16	0.9805
308	0.77	0.0195	1.36	0.9812
318	0.86	0.0285	1.37	0.9899
328	0.89	0.0354	1.41	0.9898

The pseudo-first-order model kinetic parameter (Table 1), such as the regression coefficient R^2 (values between 0.86 and 0.97), give a non-representative model for AAI adsorption behavior. The pseudo-first-order kinetic model gave values of calculated adsorption capacities, ($q_{e,calc}$.), which deviated considerably from the adsorption capacities measured during the experiments, ($q_{e,exp}$.). The experimental data were subsequently fitted to the pseudo-second-order kinetic model to evaluate its suitability in describing the adsorption process. The kinetic parameters (Table 1), especially the regression coefficient with values close to 1, gave a model of the AAI adsorption behavior. Therefore, there is a close alignment between the calculated adsorption capacities from the model and the experimental ones. The adsorption is driven by a physical mechanism, engaging the formation of physical bonds between the AAI molecules and the adsorbent surface [20].

3.2.5. Thermodynamics Studies

The thermodynamic parameters for AAI adsorption on the tested materials were obtained from the slope and intercept of the linear plot of $\ln K_d$ as a function of 1/T (Figure 6). The values of ΔG°, ΔH°, and ΔS° are shown in Table 2.



(**a**) (**b**)

Figure 6. Thermodynamics studies: (**a**) Arrhenius; (**b**) $\ln K_d$ = f(1/T).

Table 2. AAI adsorption thermodynamic parameters.

ΔH° (kJ/mol)	**ΔS° (J/mol·K)**	**ΔG° (kJ/mol)**				**R^2**
		298 K	**308 K**	**318 K**	**328 K**	
20.70	58.83	−16.02	−16.55	−17.09	−17.63	0.9881

The differences between the Gibbs free energy values indicate that the adsorption of AAI onto AC occurs spontaneously. In addition, the decrease in Gibbs free energy with rising temperature shows that higher temperatures favor the adsorption process. Positive values of standard enthalpy changes confirm the endothermic nature of the process, supported by observed increases in both the equilibrium adsorption capacity and the pseudo-second-order rate constant (k_2) as temperature increases. However, according to the literature data, if ΔH° is >20 kJ/mol, it can be stated that the process has a physicochemical nature [30]. From the positive standard entropy values, it can be interpretated that the adsorption process increases disorder at the interface between the liquid/solid phases. Because these values are relatively small, it implies that adsorption causes negligible changes in the system's disorder.

The activation energy calculated is 2.54 kJ/mol, with a correlation coefficient of 0.9928. The activation energy value indicates that the adsorption of AAI on AC is conducted by a physical adsorption mechanism [31].

3.2.6. Equilibrium Studies—Adsorption Isotherms

The adsorption mechanism of AAI on AC was calculated based on the three models: Freundlich, Langmuir, and Sips. Figure 7 shows the three equilibrium isotherms, and Table 3 shows the equilibrium isotherm parameters for AAI adsorption on AC. As the initial concentration of the AAI solution increases, the adsorption capacity also increases, reaching the maximum adsorption capacity for AC of qm, exp = 10.67 mg/g for a Ci AAI of 150 mg/L.

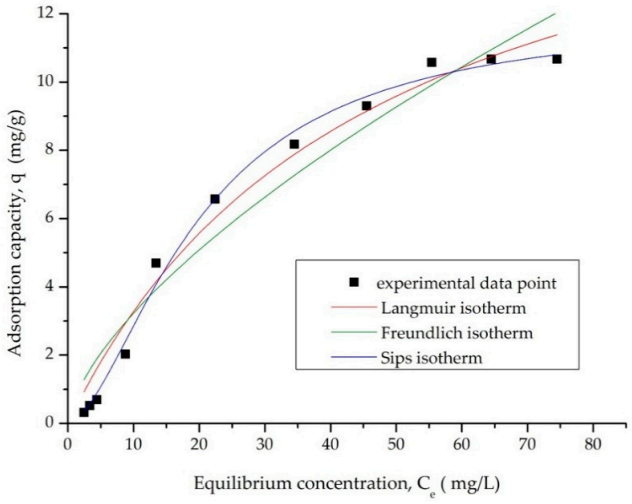


Figure 7. Equilibrium studies.

Table 3. Isotherm model parameters for the adsorption of AAI onto AC.

Langmuir Isotherm			
$q_{m,\,exp}$ (mg/g)	K_L (L/mg)	q_L (mg/g)	R^2
0.67	0.0216	18.45	0.9763
Freundlich Isotherm			
K_F (mg/g)	$1/n_F$		R^2
0.713	0.65		0.9430
Sips Isotherm			
K_S	q_S (mg/g)	$1/n_S$	R^2
0.006	11.9	0.60	0.9933

The Freundlich isotherm exhibits the lowest correlation coefficient (R^2 = 0.9430), suggesting that it provides the least accurate fit to the experimental data (Table 3). In contrast, the Sips isotherm shows a much higher correlation coefficient (R^2 = 0.9933), indicating that this model offers the best agreement with the experimental results.

4. Discussion

In this study, the physical mechanism of the toxic aristolochic acid I (AAI) adsorption on an environmentally friendly material, activated carbon (AC), was established. This process is guided by subtle interactions like van der Waals forces and hydrogen bonding, which are in line with the low activation energy values observed, as noted Van Oss et al. (1986) [32]. Adsorption studies revealed that AC exhibits a high adsorption capacity of 10.67 mg/g, surpassing the capacities reported in other studies (Table 4). As such, the adsorption is referred to as endothermic and spontaneous, indicating that high temperatures enhance the favorability and efficiency of AAI removal. Kinetic analysis establishes that the adsorption is consistent with a pseudo-second-order mechanism. This suggests that the rate of adsorption depends on the number of sites available for adsorption and most likely involves multilayer adsorption or higher-order interactions rather than simple physisorption [26]. Equilibrium data are fitted most satisfactorily by the Sips isotherm model, which incorporates some of the features of both the Langmuir (monolayer) and the Freundlich (heterogeneous, multilayer) isotherms. This model illuminates the heterogeneous adsorbent surface and enables maximum adsorption capacity and affinity prediction [33]. Kinetic, thermodynamic, and equilibrium models are employed to describe the AAI adsorption mechanism, estimate the rate and extent of adsorption, and optimize the yield of operational parameters like pH, temperature, and adsorbent dosage for effective toxin removal. These mathematical models are crucial in describing the adsorption energy profile, predicting system behavior under varying conditions, and designing practical and scalable detoxification processes [24,27].

Table 4. Maximum adsorption capacities—comparison with the literature.

Absorbents	Maximum Adsorption Capacities	Ref
Molecularly imprinted polymers (TMNIPs)	2.60 mg/g	[34]
Dummy molecularly imprinted silica material (MIS)	8.12 mg/g	[35]
Molecularly imprinted polymers (TMMIPs)	8.51 mg/g	[34]
Magnetic mesoporous carbon (MMC@MIPs)	8.65 mg/g	[36]
Molecular carbon nanotubes (MCNTs@AAI-MIPs)	18.54 mg/g	[9]
Magnetic nanocomposite (CNT/Fe_3O_4@SiO_2-AzI)	24.5 mg/g	[37]
Magnetic nanocomposite (MNs@SiO_2T-DvbDam)	37.30 mg/g	[38]
Metal–organic framework (UiO-66-NH_2)	42.74 mg/g	[39]
Chitosan-modified carbon microcoils (CMCs@CS)	77.72 mg/g	[40]
Magnetic solid phase extraction (Fe_3O_4@SiO_2-TPM@StVp)	n.d.a	[41]
AC	10.67 mg/g	This paper

n. d. a.—no data available.

Activated carbon showed a higher adsorption capacity (10.67 mg/g) than most molecularly imprinted polymers and silica-based materials yet remained below the performance of MOFs and chitosan-modified carbon microcoils. The best adsorption capacity of AAI removal was reported by Shu et al. (2018) [40], who developed chitosan-modified carbon microspirals specifically designed for the selective extraction of AAI from medicinal plants,

demonstrating outstanding binding efficiency of 77.72 mg/g and satisfactory selectivity. Recently, in 2025, Han et al. [39] synthesized a molecularly imprinted metal–organic framework UiO-66-NH2 via a one-pot hydrothermal method using indomethacin (IND), obtaining a material that facilitates highly selective recognition and efficient adsorption of AAI (42.74 mg/g), with an adsorption efficiency of over 80% after five adsorption–desorption cycles, indicating good structural stability and reusability. However, the main limitation of MOF materials is related to their instability in water, and potential biotoxicity [6,42].

Other adsorbents with suitable maximum adsorption capacity are magnetic nanocomposite (MNs@SiO_2T-DvbDam) [38] and magnetic nanocomposite (CNT/Fe3O4@SiO_2-Az) [41], while molecularly imprinted polymers (TMNIPs) [24], dummy molecularly imprinted silica material-MIS [35], molecularly imprinted polymers (TMMIPs) [36], and magnetic mesoporous carbon (MMC@MIPs) [9] presented maximum adsorption capacities inferior to the AC. The adsorption method described can be applied to obtain purified drugs without affecting their efficacy. The present results indicate that AC can be a suitable way for the removal of aristolochic acid (AAI), a toxic compound present in medicinal plant species such as *Aristolochia* and *Asarum*.

Strengths, Limitations, and Future Perspectives of the Study

The present article focuses on highlighting the physical nature of the adsorption reactions rather than on the detailed characterization of the adsorbent material, and demonstrates that the adsorption of aristolochic acid I occurs effectively on activated carbon. The strength of this study is the first-time use of a common and cheap material adsorbent, activated carbon. Activated carbon demonstrates high efficiency and eco-compatibility in adsorbing toxic aristolochic acid I. A major limitation is the selectivity of the adsorbent; therefore, further studies on this parameter need to be performed. Also, other limitations of using physical methods may be the high cost, their laborious syntheses, or their instability. Comprehensive material characterization methods, such as BET surface area, pore size and image analysis and toxicokinetic studies could be conducted in future work to offer further support and complement the current findings.

5. Conclusions

In the present paper, adsorption studies showed that AC has a good AAI adsorption capacity, at 10.67 mg/g. The adsorption mechanism was clarified through kinetic, thermodynamic, and equilibrium analyses. The findings indicate that the process is spontaneous and endothermic and the adsorption capacity increase by increasing the pH up to 6, where it stabilizes. The maximum absorption efficiency of AC was 55%, being reached at a S:L ratio of 0.2 g/25 mL. The Sips model is the model that successfully describes the adsorption process, showing the highest values for the correlation coefficient (R^2). The reaction rate is described by the pseudo-second-order model. UV-VIS spectroscopy as a method of analysis for AAI was found to be a simple but efficient method. The process of adsorption is dictated by physical forces on the heterogeneous surface, is spontaneous under controlled conditions, and can be described and optimized quantitatively using established kinetic and equilibrium models, thereby ensuring effective detoxification. The results indicate that AC can be used effectively in the removal of AAI, a toxic compound present in medicinal plant species such as *Aristolochia* and *Asarum*.

Author Contributions: Conceptualization, A.N. and C.A.T.; methodology, A.N.; software M.C. and I.B.P.; validation: C.O.; formal analysis, M.-A.P. and I.B.P.; investigation, M.C., I.-M.C. and A.I.; resources, A.N. and V.P.; data curation, M.-A.P., I.B.P. and M.C.; writing—original draft preparation, M.-A.P., C.O. and A.T.L.-G.; writing—review and editing, A.T.L.-G., C.O., A.I. and I.-M.C.; visualiza-

tion, A.N., C.A.T. and V.P.; supervision, C.A.T., A.T.L.-G. and V.P. All authors have read and agreed to the published version of the manuscript.

Funding: This research received no external funding.

Data Availability Statement: The original contributions presented in this study are included in the article. Further inquiries can be directed to the corresponding authors.

Conflicts of Interest: The authors declare no conflicts of interest.

Abbreviations

The following abbreviations are used in this manuscript:

AA	Aristolochic acid
AAs	Aristolochic acids
AAI	Aristolochic acid I
AC	Activated carbon
AAN	Aristolochic Acid Nephropathy
BEN	Balkan Endemic Nephropathy
CHN	Chinese Herbal Nephropathy
CMC	Carbon microcoils
CNT	Carbon nanotubes
EME	Electromembrane extraction
IND	Indomethacin
MIP	Molecularly imprinted polymers
MOF	Metal–Organic Frameworks
S:L	Solid/Liquid
UV-VIS	Ultraviolet–visible

References

1. Ioset, J.-R.; Raoelison, G.E.; Hostettmann, K. Detection of Aristolochic Acid in Chinese Phytomedicines and Dietary Supplements Used as Slimming Regimens. *Food Chem. Toxicol.* **2003**, *41*, 29–36. [CrossRef]
2. Ng, A.W.T.; Poon, S.L.; Huang, M.N.; Lim, J.Q.; Boot, A.; Yu, W.; Suzuki, Y.; Thangaraju, S.; Ng, C.C.Y.; Tan, P.; et al. Aristolochic Acids and Their Derivatives Are Widely Implicated in Liver Cancers in Taiwan and throughout Asia. *Sci. Transl. Med.* **2017**, *9*, eaan6446. [CrossRef]
3. Wang, C.; Liu, Y.; Han, J.; Li, W.; Sun, J.; Wang, Y. Detection and Removal of Aristolochic Acid in Natural Plants, Pharmaceuticals, and Environmental and Biological Samples: A Review. *Molecules* **2023**, *29*, 81. [CrossRef] [PubMed]
4. Wang, X.; Jiang, D.; Shi, Q.; Ren, G.; Liu, C. Microbial Degradation of Aristolochic Acid I by Endophytic Fungus A.h-Fs-1 of Asarum Heterotropoides. *Front. Microbiol.* **2022**, *13*, 917117. [CrossRef] [PubMed]
5. Fang, L.; Tian, M.; Row, K.H.; Yan, X.; Xiao, W. Isolation of Aristolochic Acid I from Herbal Plant Using Molecular Imprinted Polymer Composited Ionic Liquid-based Zeolitic Imidazolate Framework-67. *J. Sep. Sci.* **2019**, *42*, 3047–3053. [CrossRef]
6. Zhang, M.; Liu, H.; Han, Y.; Bai, L.; Yan, H. On-Line Enrichment and Determination of Aristolochic Acid in Medicinal Plants Using a MOF-Based Composite Monolith as Adsorbent. *J. Chromatogr. B* **2020**, *1159*, 122343. [CrossRef]
7. Xu, Q.; Zhou, Q.; Pan, M.; Dai, L. Interaction between Chlortetracycline and Calcium-Rich Biochar: Enhanced Removal by Adsorption Coupled with Flocculation. *Chem. Eng. J.* **2020**, *382*, 122705. [CrossRef]
8. Shu, H.; Chen, G.; Wang, L.; Cui, X.; Luo, Z.; Jing, W.; Chang, C.; Zeng, A.; Zhang, J.; Fu, Q. Metal-Organic Framework Grafted with Melamine for the Selective Recognition and Miniaturized Solid Phase Extraction of Aristolochic Acid I from Traditional Chinese Medicine. *J. Chromatogr. A* **2021**, *1647*, 462155. [CrossRef] [PubMed]
9. Li, F.; Gao, J.; Li, X.; Li, Y.; He, X.; Chen, L.; Zhang, Y. Preparation of Magnetic Molecularly Imprinted Polymers Functionalized Carbon Nanotubes for Highly Selective Removal of Aristolochic Acid. *J. Chromatogr. A* **2019**, *1602*, 168–177. [CrossRef]
10. Yan, Y.; Huang, C.; Shen, X. Electromembrane Extraction of Aristolochic Acids: New Insights in Separation of Bioactive Ingredients of Traditional Chinese Medicines. *J. Chromatogr. A* **2019**, *1608*, 460424. [CrossRef]
11. Zhang, J.; Wang, Y.; Sun, J.; Zhou, G.; Jiang, X.; Wang, X. QuEChERS Pretreatment Combined with High-Performance Liquid Chromatography-Tandem Mass Spectrometry for Determination of Aristolochic Acids I and II in Chinese Herbal Patent Medicines. *RSC Adv.* **2020**, *10*, 25319–25324. [CrossRef] [PubMed]

12. Vaclavik, L.; Krynitsky, A.J.; Rader, J.I. Quantification of Aristolochic Acids I and II in Herbal Dietary Supplements by Ultra-High-Performance Liquid Chromatography–Multistage Fragmentation Mass Spectrometry. *Food Addit. Contam. Part A* **2014**, *31*, 784–791. [CrossRef]
13. Liang, Q.; Chow, A.H.L.; Wang, Y.; Tong, H.H.Y.; Zheng, Y. Removal of Toxic Aristolochic Acid Components from Aristolochia Plants by Supercritical Fluid Extraction. *Sep. Purif. Technol.* **2010**, *72*, 269–274. [CrossRef]
14. Chan, C.-K.; Tung, K.-K.; Pavlović, N.M.; Chan, W. Remediation of Aristolochic Acid-Contaminated Soil by an Effective Advanced Oxidation Process. *Sci. Total Environ.* **2020**, *720*, 137528. [CrossRef]
15. Mohammad-Khah, A.; Ansari, R. Activated Charcoal: Preparation, Characterization and Applications: A Review Article. *Int. J. ChemTech Res.* **2009**, *1*, 859–864.
16. Mladin, G.; Ciopec, M.; Negrea, A.; Duteanu, N.; Negrea, P.; Svera, P.; Ianăşi, C. Selenite Removal from Aqueous Solution Using Silica–Iron Oxide Nanocomposite Adsorbents. *Gels* **2023**, *9*, 497. [CrossRef]
17. Iqbal, M.J.; Ashiq, M.N. Adsorption of Dyes from Aqueous Solutions on Activated Charcoal. *J. Hazard. Mater.* **2007**, *139*, 57–66. [CrossRef] [PubMed]
18. Mihăilescu, M.; Negrea, A.; Ciopec, M.; Davidescu, C.M.; Negrea, P.; Duţeanu, N.; Rusu, G. Gold (III) Adsorption from Dilute Waste Solutions onto Amberlite XAD7 Resin Modified with L-Glutamic Acid. *Sci. Rep.* **2019**, *9*, 8757. [CrossRef]
19. Lagergren, S. About the Theory of So-Called Adsorption of Solution Substances. *K. Sven. Vetenskapsakademiens Handl.* **1898**, *24*, 147–156.
20. Ho, Y. Review of Second-Order Models for Adsorption Systems. *J. Hazard. Mater.* **2006**, *136*, 681–689. [CrossRef]
21. Do, D.D. *Adsorption Analysis: Equilibria and Kinetics (with CD Containing Computer MATLAB Programs)*; World Scientific: Singapore, 1998; ISBN 978-1-78326-224-3.
22. Langmuir, I. The Adsorption of Gases on Plane Surfaces of Glass, Mica and Platinum. *J. Am. Chem. Soc.* **1918**, *40*, 1361–1403. [CrossRef]
23. Febrianto, J.; Kosasih, A.N.; Sunarso, J.; Ju, Y.-H.; Indraswati, N.; Ismadji, S. Equilibrium and Kinetic Studies in Adsorption of Heavy Metals Using Biosorbent: A Summary of Recent Studies. *J. Hazard. Mater.* **2009**, *162*, 616–645. [CrossRef]
24. Freundlich, H.M.F. Over the Adsorption in Solution. *J. Phys. Chem.* **1906**, *57*, 1100–1107.
25. Sips, R. On the Structure of a Catalyst Surface. *J. Chem. Phys.* **1948**, *16*, 490–495. [CrossRef]
26. El-Khaiary, M.I.; Malash, G.F. Common Data Analysis Errors in Batch Adsorption Studies. *Hydrometallurgy* **2011**, *105*, 314–320. [CrossRef]
27. Foo, K.Y.; Hameed, B.H. Insights into the Modeling of Adsorption Isotherm Systems. *Chem. Eng. J.* **2010**, *156*, 2–10. [CrossRef]
28. Joshi, B.D.; Srivastava, A.; Gupta, V.; Tandon, P.; Jain, S. Spectroscopic and Quantum Chemical Study of an Alkaloid Aristolochic Acid I. *Spectrochim. Acta Part A Mol. Biomol. Spectrosc.* **2013**, *116*, 258–269. [CrossRef]
29. Wu, X.; Liu, J.; Huang, H.; Xue, W.; Yao, X.; Jin, J. Interaction Studies of Aristolochic Acid I with Human Serum Albumin and the Binding Site of Aristolochic Acid I in Subdomain IIA. *Int. J. Biol. Macromol.* **2011**, *49*, 343–350. [CrossRef]
30. Zhang, Y.; Yu, F.; Cheng, W.; Wang, J.; Ma, J. Adsorption Equilibrium and Kinetics of the Removal of Ammoniacal Nitrogen by Zeolite X/Activated Carbon Composite Synthesized from Elutrilithe. *J. Chem.* **2017**, *2017*, 1936829. [CrossRef]
31. Nasiri, H.; Salahandish, M.; Sharifi, H.; Mohammadzadehasl, N. Dependence of Extinction Cross-Section, Absorption and Surface Plasmon Resonance of Nanoparticle Surface Size and Concentration of Silica@Gold Nanoparticles. *Biomed. Mater. Devices* **2025**, *3*, 1501–1508. [CrossRef]
32. Van Oss, C.J.; Good, R.J.; Chaudhury, M.K. The Role of van Der Waals Forces and Hydrogen Bonds in "Hydrophobic Interactions" between Biopolymers and Low Energy Surfaces. *J. Colloid. Interface Sci.* **1986**, *111*, 378–390. [CrossRef]
33. Ehiomogue, P.; Ahuchaogu, I.I.; Ahaneku, I.E. Review of Adsorption Isotherms Models. *Acta Tech. Corviniensis Bull. Eng.* **2021**, *14*, 87–96.
34. Xiong, H.; Fan, Y.; Mao, X.; Guo, L.; Yan, A.; Guo, X.; Wan, Y.; Wan, H. Thermosensitive and Magnetic Molecularly Imprinted Polymers for Selective Recognition and Extraction of Aristolochic Acid I. *Food Chem.* **2022**, *372*, 131250. [CrossRef] [PubMed]
35. Wang, L.; Zhang, C.; Chen, Y.; Deng, Q.; Wang, S. Dummy Molecularly Imprinted Silica Materials for Effective Removal of Aristolochic Acid I from Kaempfer Dutchmanspipe Root Extract. *Microchem. J.* **2020**, *152*, 104463. [CrossRef]
36. Ge, Y.-H.; Shu, H.; Xu, X.-Y.; Guo, P.-Q.; Liu, R.-L.; Luo, Z.-M.; Chang, C.; Fu, Q. Combined Magnetic Porous Molecularly Imprinted Polymers and Deep Eutectic Solvents for Efficient and Selective Extraction of Aristolochic Acid I and II from Rat Urine. *Mater. Sci. Eng. C Mater. Biol. Appl.* **2019**, *97*, 650–657. [CrossRef]
37. Shu, H.; Chen, G.; Wang, L.; Cui, X.; Wang, Q.; Li, W.; Chang, C.; Guo, Q.; Luo, Z.; Fu, Q. Adenine-Coated Magnetic Multiwalled Carbon Nanotubes for the Selective Extraction of Aristolochic Acids Based on Multiple Interactions. *J. Chromatogr. A* **2020**, *1627*, 461382. [CrossRef]
38. Xie, Q.-Y.; Chen, Y.; Li, C.-J.; Zhang, J.-B.; Cao, X.-J.; Lu, J. Ionizable Copolymer Functionalized Magnetic Nanocomposite as an Adsorbent for Boosting the Extraction Selectivity of Aristolochic Acids. *J. Food Drug Anal.* **2024**, *32*, 65–78. [CrossRef] [PubMed]

39. Han, X.; Wang, S.; Cui, T.; Yang, Y.; Li, H.; Zhang, H.; Zhou, H.; Li, X. Sustainable Defect-Engineered Imprinted UiO-66-NH2 for Selective Removal of Aristolochic Acids from Medicinal Herbs. *ACS Sustain. Chem. Eng.* **2025**, *13*, 11113–11127. [CrossRef]
40. Shu, H.; Ge, Y.; Xu, X.-Y.; Guo, P.-Q.; Luo, Z.-M.; Du, W.; Chang, C.; Liu, R.-L.; Fu, Q. Hybrid-Type Carbon Microcoil-Chitosan Composite for Selective Extraction of Aristolochic Acid I from Aristolochiaceae Medicinal Plants. *J. Chromatogr. A* **2018**, *1561*, 13–19. [CrossRef]
41. Ji, F.; Jin, R.; Luo, C.; Deng, C.; Hu, Y.; Wang, L.; Wang, R.; Zhang, J.; Song, G. Fast Determination of Aristolochic Acid I (AAI) in Traditional Chinese Medicine Soup with Magnetic Solid-Phase Extraction by High Performance Liquid Chromatography. *J. Chromatogr. A* **2020**, *1609*, 460455. [CrossRef]
42. Gao, Q.; Bai, Q.; Zheng, C.; Sun, N.; Liu, J.; Chen, W.; Hu, F.; Lu, T. Application of Metal-Organic Framework in Diagnosis and Treatment of Diabetes. *Biomolecules* **2022**, *12*, 1240. [CrossRef] [PubMed]

Disclaimer/Publisher's Note: The statements, opinions and data contained in all publications are solely those of the individual author(s) and contributor(s) and not of MDPI and/or the editor(s). MDPI and/or the editor(s) disclaim responsibility for any injury to people or property resulting from any ideas, methods, instructions or products referred to in the content.